Electronic structure and thermoelectric transport properties of AgTlTe: First-principles calculations

M. W. Oh,[1,*] D. M. Wee,[2] S. D. Park,[1] B. S. Kim,[1] and H. W. Lee[1]
[1]*Advanced Materials and Application Research Laboratory, Korea Electrotechnology Research Institute, 28-1 Sungju-dong, Changwon 641-120, Republic of Korea*
[2]*Department of Materials Science and Engineering, Korea Advanced Institute of Science and Technology, 373-1 Guseong-dong, Yuseong-gu, Daejeon 305-701, Republic of Korea*
(Received 2 April 2007; revised manuscript received 15 January 2008; published 14 April 2008)

In this study, the electronic structure of AgTlTe has been studied with first-principles calculations. The density of states and band structure were studied in detail. The thermoelectric power, electrical conductivity, and electronic thermal conductivity were analyzed using the Boltzmann transport equation with the assumption of the constant relaxation time approximation and the rigid band model. By using the calculated thermoelectric properties and experimental thermal conductivity, the dimensionless figure of merit *ZT* was obtained. The enhancement of the thermoelectric properties of AgTlTe by adjusting carrier concentration is predicted.

DOI: 10.1103/PhysRevB.77.165119 PACS number(s): 72.15.Jf, 71.15.Mb, 72.10.Bg

I. INTRODUCTION

Thermoelectric devices have attracted much interest as they can be used for small-scale cooling applications and for power generation in remote areas and in outer space. The efficiency of a thermoelectric device depends on its geometry and the dimensionless thermoelectric figure of merit *ZT* of the materials that constitute the device.[1] The *ZT* is defined by the following equation:

$$ZT = (S^2\sigma/\kappa)T, \tag{1}$$

where σ is the electrical conductivity, S is the thermoelectric power, κ is the thermal conductivity, and T is the temperature measured in Kelvin.[2] In the past, many thermoelectric materials with $ZT \sim 1$ were developed, but these values of *ZT* were insufficient for use in commercial refrigeration or power generation applications.[1] The definition of *ZT* suggests that σ and S should be enhanced, while κ should be reduced in order to maximize *ZT* values. κ consists of an electronic contribution κ_e and a phonon contribution κ_{ph}. It is initially necessary to find materials that have a low κ value to develop a noble high-performance thermoelectric material.

The ternary compounds of *X*-Tl-Te (*X*=Ag, Bi, Sn, and Ge) have extremely low thermal conductivity values, with most thermal conduction given by the phonons.[3–7] For instance, the values of κ_{ph} are 0.39, 0.23, and 0.25 W/mK at 300 K for Tl_9BiTe_6,[3] Ag_9TlTe_5, and AgTlTe,[5,7] respectively. The maximum *ZT* values of these compounds are $ZT=1.2$ at approximately 500 K for Tl_9BiTe_6,[3] $ZT=1.23$ at 700 K for Ag_9TlTe_5,[5] and $ZT=0.61$ at 600 K for AgTlTe.[3,5,6] It is possible to control the carrier concentration by using doping to improve the thermoelectric properties, but attempts to do this are not reported in the literature for these compounds.

The thermoelectric properties, σ, S, and κ_e, are directly related to the electronic structure of the material. Recently, a prediction of the thermoelectric properties from first-principles calculations was shown to be in good agreement with experimental results for many well-known thermoelectric materials.[8,9] This type of theoretical approach can also be utilized for Tl-Te compounds. To the best of the authors' knowledge, a study of the electronic structure of AgTlTe has not yet been reported. In this study, the electronic structure of AgTlTe is calculated within the framework of density-functional theory. Unfortunately, the crystal structures of the other ternary compounds, such as Tl_9BiTe_6 and Al_9TlTe_6, are too complex for a calculation of their electronic structures. The calculated electronic structure is then used to calculate the transport properties of AgTlTe. The transport properties are calculated with a large number of k points in the Brillouin zone by using the Boltzmann transport theory.

II. COMPUTATIONAL DETAILS

The total-energy calculation and full structural optimization were performed using the Vienna *ab initio* simulation package (VASP).[10] Projector augmented-wave pseudopotentials were used.[11] The exchange and correlation were treated within the generalized gradient approximation (GGA).[12] The size of the k mesh was chosen to be $9\times16\times10$ for the conventional cell. To assure convergence of the energy, a cutoff value of 330 eV was used. It was found that the convergence in the total energy was better than 1 meV/atom by using this cutoff energy and k-mesh grid. Total-energy minimization via a lattice parameter optimization and atomic position relaxation in a conjugate gradient routine was obtained by calculating the Hellmann–Feynman forces, which are reduced to within the 0.01 eV/Å for each atom. The electronic structure was calculated with the structural parameters fully optimized by the VASP code.

The electronic structures were calculated using L/APW+lo method as implemented in the WIEN2k code.[13] The sphere sizes were 2.5 a.u. (1 a.u.=1 Bohr radius) for all atoms. The plane-wave cutoff was defined by $R_{MT}k_{MAX}=10$, which gives good convergence. Within the whole Brillouin zone, 200 k points were used during the self-consistency cycle. The exchange correlation potential was computed with the Perdew–Burke–Ernzerhof GGA within the density-functional theory.[12] The spin-orbit interaction (SOI) was incorporated using a second variational procedure.[14]

TABLE I. Experimental and calculated crystal structures.

		Experimental[a]			Calculated		
Lattice parameters (Å)		*a*	*b*	*c*	*a*	*b*	*c*
		8.754	4.854	7.750	8.865	4.938	7.893
		x	*y*	*z*	*x*	*y*	*z*
Atomic positions	Ag	0.1613	0.25	0.5794	0.1613	0.25	0.5794
	Tl	0.4899	0.25	0.3254	0.4898	0.25	0.3255
	Te	0.3141	0.25	0.8933	0.3143	0.25	0.8937

[a]Reference 17.

The Boltzmann transport equation and the rigid band approach were used to calculate the transport properties. The details of the calculation procedure are reviewed in the literature.[15] Therefore, in this paper, we only briefly introduce the primary concepts. The electrical conductivity tensor $\boldsymbol{\sigma}$ is given as

$$\sigma(\varepsilon) = \frac{e^2}{N\Omega}\int d\varepsilon\left(-\frac{\partial f_0}{\partial \varepsilon}\right)\sum_{n,k}\tau_{n,k}\vec{v}_{n,k}\vec{v}_{n,k}\delta(\varepsilon-\varepsilon_{n,k}), \quad (2)$$

where e is the charge of the carrier, N is the number of k points used in the calculation, Ω is the volume of the unit cell, f_0 is the equilibrium Fermi–Dirac distribution function, $\tau_{n,k}$ is the relaxation time, $\vec{v}_{n,k}$ denotes the group velocity, $\varepsilon_{n,k}$ stands for the band energy, and δ is the delta function. The subscripts n and k denote the band index and a crystal momentum in the case of a crystalline solid, respectively. $\vec{v}_{n,k}$ can be derived from the band structure using the following relationship:

$$\vec{v}_{n,k} = \frac{1}{\hbar}\frac{\partial \varepsilon_{n,k}}{\partial k}. \quad (3)$$

The thermoelectric power tensor $\boldsymbol{S}$ can be defined as

$$\boldsymbol{S} = \frac{ek_B}{N\Omega}\sigma^{-1}\int d\varepsilon\left(-\frac{\partial f_0}{\partial \varepsilon}\right)\left(\frac{\varepsilon-\mu}{k_BT}\right)\sum_{n,k}\tau_{n,k}\vec{v}_{n,k}\vec{v}_{n,k}\delta(\varepsilon-\varepsilon_{n,k}), \quad (4)$$

where k_B is Boltzmann's constant, μ is the chemical potential, and T is the temperature. In order to obtain $\boldsymbol{\sigma}$ and $\boldsymbol{S}$, the relaxation time τ has to be approximated. In principle, the relaxation time is dependent on the band energy $\varepsilon_{n,k}$. However, it is assumed that the relaxation time is constant. This assumption is often used in the calculation of transport properties and actually proves to be a good approximation.[9,15,16]

The electronic thermal conductivity κ_e can be defined as

$$\kappa_e = \frac{{k_B}^2T}{N\Omega}\int d\varepsilon\left(-\frac{\partial f_0}{\partial \varepsilon}\right)\left(\frac{\varepsilon-\mu}{k_BT}\right)^2\sum_{n,k}\tau_{n,k}\vec{v}_{n,k}\vec{v}_{n,k}\delta(\varepsilon-\varepsilon_{n,k}) - T\sigma\boldsymbol{S}^2. \quad (5)$$

For the transport calculation, eigenenergies were calculated for 36 000 k points for AgTlTe. A smoothed Fourier interpolation was used to obtain the analytical expression of the bands. The mesh was interpolated onto a mesh five times as dense as the original.

III. RESULTS AND DISCUSSION

The crystal structure of AgTlTe is orthorhombic with the space group *Pnma* (No. 62).[17] Computational results for structural parameters are summarized in Table I. The calculated values are in good agreement with the experimental values within 2%. The atomic positions for all elements were scarcely changed.

The calculated density of states (DOS) of AgTlTe is shown in Fig. 1. In order to observe the effect of the SOI, the DOS results were plotted with and without SOI. It was found that the conduction band minimum (CBM) with SOI is shifted downward by 0.22 eV relative to the top of the valence band as compared with CBM without SOI. This type of shift is also found in In-doped PbTe systems.[18] Otherwise, the valence band maximum (VBM) was scarcely affected by the SOI.

The band structure of AgTlTe is shown in Fig. 2. It is observable that the VBM lies at $k=2\pi(0.21a^*,0,0)$ in reciprocal lattice vectors along the Γ-X line. It is noticeable that the band edge at the Γ point is found just below the VBM. The CBM is located at the T point $[k=2\pi(0,1/2b^*,1/2c^*)]$. Due to the symmetry, this band edge yields four electron pockets. It is interesting to note that a

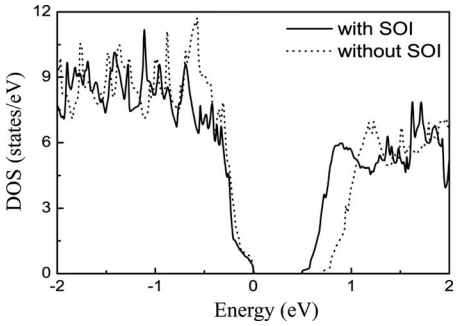

FIG. 1. Calculated density of states of AgTlTe with and without spin-orbit interactions.

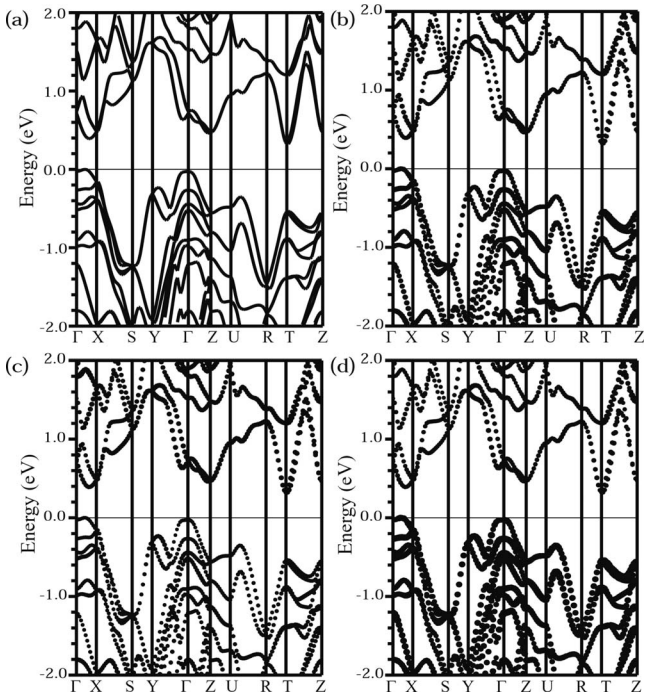

FIG. 2. Band structure of AgTlTe with the SOI. Included are (a) the total band structure and orbital character contribution of the band: (b) Ag atom, (c) Tl atom, and (d) Te atom. The size of the circle is proportional to the contribution of each atom to the total band structure. The valence band maximum is set to 0.

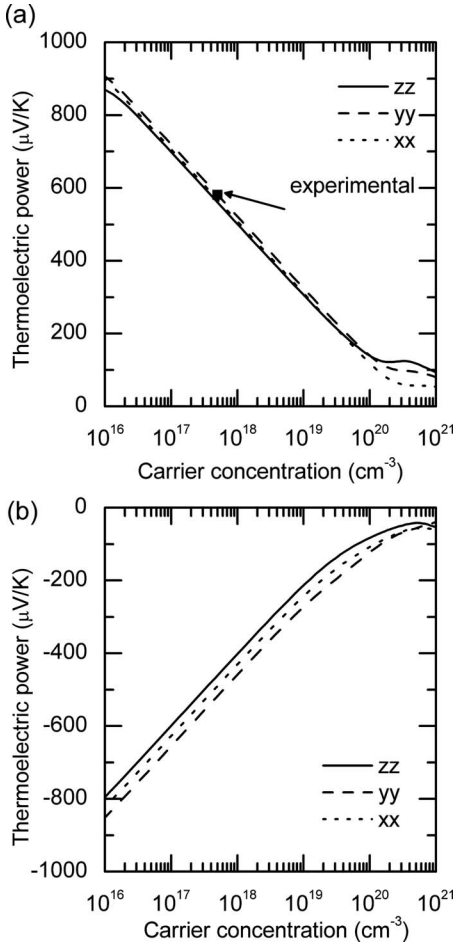

FIG. 3. Calculated values of the thermoelectric power at 300 K from the band structure of AgTlTe as a function of the carrier concentration of (a) holes and (b) electrons. The experimental result (Ref. 21) is included in the plot.

further electron pocket just above the CBM is found at $k=2\pi(0.32a^*,0,0)$ along the Γ-X line, which is denoted as cv1. The electron pocket, cv1, is 0.07 eV higher than the CBM. An additional electron pocket is located at the Z point $[k=2\pi(0,0,1/2c^*)]$, which is 0.07 eV higher than cv1. Note that the energy band approximately 0.1 eV above and below the chemical potential is included in the transport at 300 K since the function of $\partial f(\varepsilon)/\partial\varepsilon$ in Eqs. (2) and (4) plays as an energy-window function. Thus, these electron pockets may be included in the transport process at the given chemical potential. The details of the band structure mentioned above show the multivalley band structure of AgTlTe. The multivalley structure is thought to be favorable for thermoelectricity.[8,19] Based on the multivalley band structure of AgTlTe, AgTlTe may be considered as a candidate for the best thermoelectric materials. Without the SOI, the cv1 pocket was found at the X point. The shift of the pocket from the symmetry point to a position lying between the symmetry positions, as caused by the SOI, is also found in Bi_2Te_3.[20] The effect of the SOI is very important in compounds, with constituent elements that are very heavy. The indirect band gap between the CBM and the VBM is 0.32 eV. As is shown in Figs. 2(b)–2(d), the CBM has different contributions from all the atoms, but the VBM has a large amount from the Te atoms.

Under the assumption of a constant relaxation time, the thermoelectric power can be calculated without any fitting parameter. The calculated thermoelectric power is plotted as a function of the carrier concentration in Fig. 3. The calculated values from Eq. (4) are dependent on the chemical potential and the temperature. Since the carrier concentration can be estimated from the chemical potential in the rigid band model, the properties are plotted as a function of the carrier concentration. The calculation is performed at $T=300$ K and the temperature dependence of the band structure is neglected. The validity of the calculations can be estimated by comparing them with the experimental data. The experimental value of the thermoelectric power at 300 K for AgTlTe single crystals is also included in Fig. 3. The experimental value of the thermoelectric power for AgTlTe single crystal was approximately 580 μV/K at 300 K.[21] The measured concentration of the carrier (holes) was about 5×10^{17} cm^{-3} at 300 K. Note that the measuring direction for the transport properties was not mentioned in Ref. 21. However, the agreement between the experiment and theory is very good.

In contrast to the thermoelectric power, in order to quantitatively calculate the electrical conductivity, an estimation of the relaxation time is needed. The experimental value of the electrical conductivity is about 245 $(\Omega\ m)^{-1}$ with the carrier concentration of 5×10^{17} cm^{-3}.[21] As mentioned earlier, because the measuring direction in the experiment was not informed in Ref. 21, it was hard to estimate the relaxation

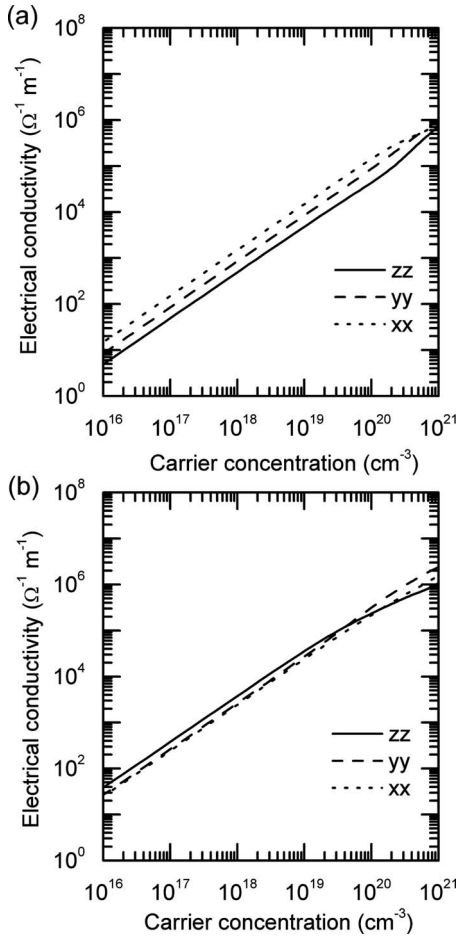

FIG. 4. Calculated values of the electrical conductivity at 300 K from the band structure of AgTlTe at 300 K as a function of the carrier concentration of (a) holes and (b) electrons.

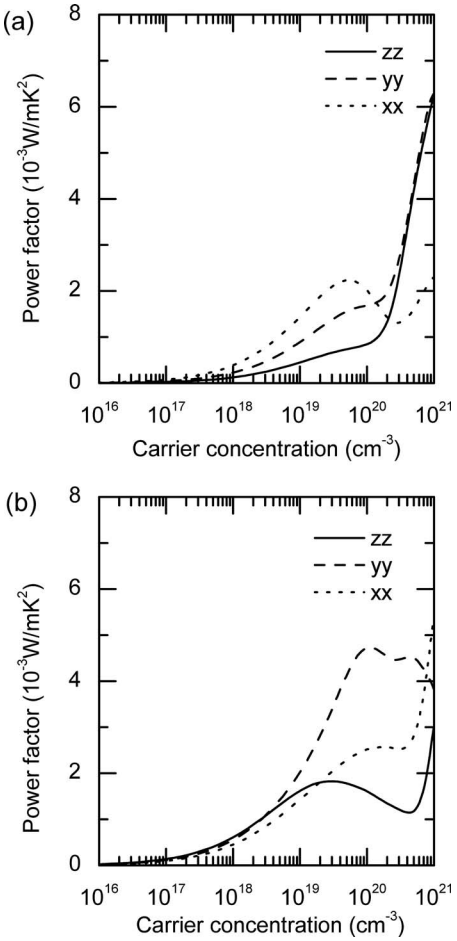

FIG. 5. Calculated values of the power factor at 300 K from the band structure of AgTlTe at 300 K as a function of the carrier concentration of (a) holes and (b) electrons.

time from fitting the calculated value with the experimental value. The calculated electrical conductivity with the value of $\tau=2.2\times10^{-14}$ s is plotted as a function of the concentration in Fig. 4. The value of $\tau=2.2\times10^{-14}$ s is chosen so that the calculated value of the electrical conductivity along the *zz* direction is fitted to the experimental value. If the measuring direction is assumed to be along the *yy* and *xx* directions, the values of $\tau=1.28\times10^{-14}$ s and $\tau=7.2\times10^{-15}$ s show the best agreement with the experiment, respectively. Due to the lack of information on the measuring direction, the anisotropy of the relaxation time is difficult to discuss. The directional electrical transport properties should be measured in order to estimate the anisotropy. In principle, the relaxation times of electrons and holes are not the same. However, because there is no report on the electrical properties for *n*-type doped AgTlTe, the relaxation time cannot be estimated from fitting the experimental data. To compare with the *p*-type one, the value of $\tau=2.2\times10^{-14}$ s is used to calculate the electrical conductivity for the *n*-type one.

The power factor σS^2 can be derived from the calculated thermoelectric power and electrical conductivity. Figure 5 shows the estimated power factor along the crystal directions at 300 K. The value of $\tau=2.2\times10^{-14}$ s is used in the estimation. The power factors for both *p*- and *n*-type materials increase as the carrier concentration increase in the range between 10^{17} and about 10^{20} cm^{-3}. This is due to the fact that the electrical conductivity largely increases as the concentration increases. The choice of the value of τ does not alter the behavior that the power factor increase with the increase in the concentration. Note that the concentrations in the experiment are on the order of 10^{17} cm^{-3}. It is expected that the power factor can be improved by increasing the carrier concentration. It is well known that in order to have the maximum power factor, the materials should have a carrier concentration on the order of $10^{19}-10^{20}$ cm^{-3}. It is noticeable that τ can vary with the concentration, which may alter the behavior of the power factor. Thus, the experimental study of the transport properties of AgTlTe with the various carrier concentrations is needed to confirm the theoretical estimation. Recently, it is reported that the power factor of polycrystalline $Ag_{1-x}Cu_xTlTe$ was improved as the carrier concentration increased.[22] This report partly proves the theoretical prediction.

In order to estimate the value of *ZT*, the lattice thermal conductivity κ_{ph} has to be determined. However, there is no report on the κ_{ph} of a AgTlTe single crystal. The constant value of $\kappa=0.4$ W/mK, which is the value of total thermal conductivity at 300 K for a AgTlTe single crystal, is chosen

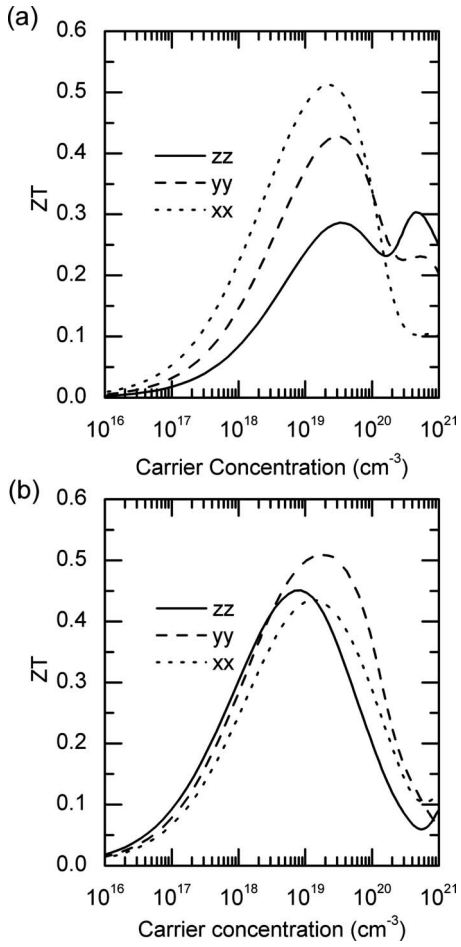

FIG. 6. Calculated values of *ZT* at 300 K from the band structure of AgTlTe as a function of the carrier concentration of (a) holes and (b) electrons.

for the estimation of *ZT*.[21] As shown in Eq. (5), τ should be chosen to estimate κ_e. The value of $\tau=2.2\times10^{-14}$ s is used for calculating κ_e. Figure 6 shows the calculated *ZT* as a function of the carrier concentration. The estimation of thermoelectric transport properties from the electronic structure says that the tuning of the carrier concentration and the utilization of the anisotropy can improve the *ZT* of AgTlTe. The improvement in *ZT* by tuning the concentration was partly proved by experiment.[22] However, the anisotropy of τ should be examined before utilizing the anisotropy, because the estimation of *ZT* was performed with the isotropic relaxation time.

IV. CONCLUSIONS

In summary, first-principles calculations were performed on the electronic structure, and the thermoelectric transport properties of AgTlTe were estimated. The fully optimized crystal structure of AgTlTe was in good agreement with the experimental results. The electronic structure was calculated with the fully optimized structure. The SOI mainly affects the lower-energy region of the conduction band, which leads to the reduction of the band gap. A band gap of 0.32 eV was obtained using a calculation with the SOI. The estimation of the thermoelectric transport properties was performed using the Boltzmann transport equation with the assumption of a constant relaxation time and a rigid band model. The calculated thermoelectric power is in quantitative agreement with experiment. The electrical conductivity is calculated with an isotropic relaxation time. By using the calculated thermoelectric power, the electrical conductivity, and the electronic thermal conductivity, the values of *ZT* along the crystallographic orientations are predicted as a function of the carrier concentration. It is predicted that the power factor can be improved by optimizing the carrier concentration and the utilization of the anisotropy, which leads to the enhancement of *ZT*. However, this prediction should be carefully applied due to the limitations of the constant relaxation time approximation and the availability of anisotropy in the relaxation time.

ACKNOWLEDGMENTS

Financial support from the Korea Energy Management Corporation and from the Korea Electrotechnology Research Institute is acknowledged.

*Author to whom correspondence should be addressed.
minwookoh@keri.re.kr

[1] B. C. Sales, Science **295**, 1248 (2002).
[2] H. J. Goldsmid, in *CRC Handbook of Thermoelectrics*, edited by D. M. Rowe (CRC, Boca Raton, FL, 1995), pp. 19–25.
[3] B. Wolfing, C. Kloc, J. Teubner, and E. Bucher, Phys. Rev. Lett. **86**, 4350 (2001).
[4] J. W. Sharp, B. C. Sales, D. Mandrus, and B. C. Chakoumakos, Appl. Phys. Lett. **74**, 3794 (1999).
[5] K. Kurosaki, A. Kosuga, H. Muta, M. Uno, and S. Yamanaka, Appl. Phys. Lett. **87**, 061919 (2005).
[6] K. Kurosaki, A. Kosuga, K. Goto, H. Muta, and S. Yamanaka, in *Proceedings of the 24th International Conference on Thermoelectrics*, 19–23 June, 2005 (IEEE, New Jersey, 2005), p. 323.
[7] K. Kurosaki, H. Uneda, H. Muta, and S. Yamanaka, J. Alloys Compd. **395**, 304 (2005).
[8] T. Thonhauser, T. J. Scheidemantel, J. O. Sofo, J. V. Badding, and G. D. Mahan, Phys. Rev. B **68**, 085201 (2003).
[9] T. J. Scheidemantel, C. Ambrosch-Draxl, T. Thonhauser, J. V. Badding, and J. O. Sofo, Phys. Rev. B **68**, 125210 (2003).
[10] G. Kresse and J. Hafner, Phys. Rev. B **47**, R558 (1993); **49**, 14251 (1994).
[11] P. E. Blochl, Phys. Rev. B **50**, 17953 (1994).
[12] J. P. Perdew, K. Burke, and M. Ernzerhof, Phys. Rev. Lett. **77**, 3865 (1996).
[13] P. Blaha, K. Schwarz, G. K. H. Madsen, D. Kvasnicka, and J. Luitz, WIEN2K, An Augmented Plane Wave Plus Local Orbitals Program for Calculating Crystal Properties, Vienna University

of Technology, Austria, 2001.
[14] J. Kuneš, P. Novák, R. Schmid, P. Blaha, and K. Schwarz, Phys. Rev. B **64**, 153102 (2001).
[15] G. K. H. Madsen and D. J. Singh, Comput. Phys. Commun. **175**, 67 (2006).
[16] P. B. Allen, W. E. Pickett, and H. Krakauer, Phys. Rev. B **37**, 7482 (1988).
[17] R. M. Ayral-Marin, B. Liautard, M. Maurin, J. C. Tedenac, and G. Brun, J. Phys. Chem. Solids **49**, 939 (1988).
[18] S. Ahmad, K. Hoang, and S. D. Mahanti, Phys. Rev. Lett. **96**, 056403 (2006).
[19] G. S. Nolas, J. Sharp, and H. J. Goldsmid, *Thermoelectrics* (Springer, Berlin, 2001), Chap. 3.
[20] P. Larson, S. D. Mahanti, and M. G. Kanatzidis, Phys. Rev. B **61**, 8162 (2000).
[21] B. Pistoulet, D. Coquillat, J. C. Tedenac, G. Brun, and M. Maurin, Phys. Status Solidi A **77**, 669 (1983).
[22] K. Kurosaki, K. Goto, H. Muta, and S. Yamanaka, J. Appl. Phys. **102**, 023707 (2007).